Minerals Engineering 121 (2018) 122–128

Contents lists available at ScienceDirect

Minerals Engineering

journal homepage: www.elsevier.com/locate/mineng

Bioleaching process for silver recovery: Structural and rheological studies

D.M. Núñez Ramírez[a,*], L. Medina-Torres[b], F. Calderas[c], René H. Lara[d], H. Medrano Roldán[e], O. Manero[a]

[a] Instituto de Investigaciones en Materiales, Universidad Nacional Autónoma de México, México 04510, Mexico
[b] Facultad de Química, Universidad Nacional Autónoma de México, México 04510, Mexico
[c] Facultad de Estudios Superiores Zaragoza, Universidad Nacional Autónoma de Mexico, Batalla 5 de mayo S/N, Ejercito de Oriente, Iztapalapa, 09230 Ciudad de Mexico, Mexico
[d] Facultad de Ciencias Químicas, Universidad Juárez del Estado de Durango (UJED), Avenida Veterinaria, s/n, Circuito Universitario, C.P. 34120 Durango, Dgo., Mexico
[e] Innovación Tecnológica en Alimentos y Biotecnología Industrial, Instituto Tecnológico de Durango, Av. Felipe Pescador 1830 Ote, 34080 Durango, Dgo., Mexico

ARTICLE INFO

Keywords:
Minerals
Extraction
Bioleaching
Rheology and viscoelastic behavior

ABSTRACT

In this work, we characterize the microstructural and rheological properties of silver manganese mineral pulps during a bioleaching process in a continuous stirred-tank reactor (CSTR). Analysis of the dissolution kinetics of Manganese in the pulp during the bioleaching process reveals a dissolution level of 20–23% during 36–48 h. This percentage allows the extraction of large percentages of silver (Ag) during the cyanidation process, thus obtaining 64 wt% of Ag. The maximum value of viscosity attained in the medium (especially between 48 and 72 h) is an important parameter, since it may cause processing setbacks such as in-homogeneous agitation and increase in transport energy. Several factors contribute to the continuous change of viscosity in the media such as mineral wearing, the presence of the excreted bacterial exopolysaccharide (EPS), pH changes, particle size modifications due to mineral wear (plus corrosion) and changes in density of the medium. For this reason, it is of great importance to monitor the rheological behavior of the mineral pulp during the bioleaching and cyanidation processes. The mineral pulp behaves as a weak gel as reported in linear viscoelastic measurements.

1. Introduction

In recent years, the mineral industry has shifted to the mining of low-grade ores due to the depletion of conventional high-grade ores. For low-grade ores resources, biological processing can be economically more effective and an environmentally friendlier alternative to traditional hydro-metallurgical and pyro-metallurgical processes (Sandström y Petersson, 1997; Erüst et al., 2013). Bio-hydrometallurgy is a rapidly evolving biotechnology that has already provided rooted solutions to old problems associated with the recovery of metals by conventional pyro-metallurgy or chemical metallurgy (Erüst et al., 2013). Bioleaching is a technique used for the extraction of valuable minerals from low-grade ores, involving a two-phase suspension of solid particles (mineral pulp) in a liquid medium. The rheological properties of this suspension are continuously changing in time as the bioleaching process evolves, due to growing of bacteria population, changes in solid concentration, particle size, particle size distribution, particle anisotropy, pH and material properties. Mineral particles in the suspensions are usually non-spherical, exhibiting anisotropic surface charge, thereby causing a complex rheological behavior (non-Newtonian flow, yield stresses, time dependent properties, and so on. Boger, 2000; He et al., 2004). The rheological characterization of mineral pulps is an important and essential factor to establish optimum parameters for bioleaching, and hence for the mineral industry, where highly concentrated suspensions are often encountered (Boger, 2000; Sofrá and Boger, 2002). Patra et al. (2010) reported on the impact of pulp rheology on selective recovery of Ni and Cu ores, and found that factors such as shape, size and surface chemical properties of mineral particles affect pulp rheology. Ndlovu et al. (2011) studied the influence of two phyllosilicate minerals on the rheology of mineral slurries. A complex rheological behavior of these systems arises due to the anisotropy in the surface charge and inter-particle orientation of the edges and faces of the non-spherical mineral particles in solution. Nosrati et al. (2011) studied the rheology of aging aqueous muscovite clay dispersions and found transient rheological behavior and microstructure evolution of the dispersions during aging. In addition, they observed thixotropy, yield stress, viscoelastic gel and strong rheopectic behavior. Upon aging, the dispersions show a significant attenuation of the rheological parameters although they retain their predominant elastic properties. Zhang and Peng (2015) investigated the effect of clay

* Corresponding author at: Facultad de Ciencias Químicas – UJED, Av. Veterianaria S/N, Circuito Universitario, C.P. 34120 Durango, Dgo., Mexico.
E-mail address: diolamarina@ujed.mx (D.M. Núñez Ramírez).

https://doi.org/10.1016/j.mineng.2018.03.019
Received 16 August 2017; Received in revised form 14 February 2018; Accepted 13 March 2018
Available online 21 March 2018
0892-6875/

minerals on pulp rheology and observed that clay minerals modify pulp rheology according to the type of minerals. Nonetheless, scarce literature is available to analyze the connection of the rheological properties of the system with the production of extracellular polymeric substances (exopolysaccharides, EPS) by bacteria during the bioleaching process. EPSs are mainly composed of polysaccharides and proteins, and form different structures that attach to the cell outer surface or they secrete into the growing medium, in fact, forming biofilms (Ruas-Madiedo y de los Reyes-Gavilán, 2005). These structures are affected by particle size and particle size distribution (Cerpa et al., 1999, 2001; Pérez, 2004; Rivas and Colás, 2005), particle concentration and the mineralogical properties of the dispersed phase (Zamora, 2003), particle surface chemical properties and pH of the growing medium (Cerpa and Garcell, 1998; Garcell, 2001, 2004). Since a wealth of factors affect the rheology of a bioleaching process, a systematic analysis can achieve better understanding of the rheological properties of these systems in order to improve the recovery percentage upon minimizing operational failures associated with transport and pulp concentration. Efficiency parameters based on the rheological properties are then necessary, considering that as the bioleaching process evolves, the viscosity of the mineral pulp increases, complicating the washing operations for recovery of valuable minerals (for example cyanidation) which reduces the recovery efficiency.

Based on the above premises, in this work we characterize the microstructural and rheological properties of silver manganese mineral pulps during the bioleaching process.

2. Experimental

2.1. Materials and reagents

Samples of manganese silver minerals used in this study were provided by the First Majestic Silver Corp. Metallurgical Laboratory, corresponding to the cyanidation tails of the Encantada plant. Initially the ore has a head law of 331.5 g/t Ag and 3.1 wt% Mn. Cyanidation obtains only 60% of Ag dissolution, leaving a residue or tail grade of 130 g/t Ag and 2.7% Mn. This residue or tail law is what we use for the bioleaching tests and subsequent cyanidation. Mineral compositions of the ores tails (residue) are analyzed using quantitative X-ray diffraction (XRD) as shown in Table 1. The sample is mainly composed of calcite, with small amounts of quartz, hematite, goethite, loseyite, kaolinite, and nepheline (Na, K) $AlSiO_4$, and trace amounts of Pb, Mn, Fe, Zn oxides or their respective carbonates.

Table 2 discloses the elemental compositions of the ore.

2.2. Silver, mineralogy

Heavy liquid separation (HLS) at the specific gravity of 2.9 g/cm^3 and 3.1 g/cm^3 pre-concentrates the as-received samples, following by further concentration of the sink fraction by super-panning (SP). At this stage, we only observe few mineral grains of silver, wherein the major silver carriers are pyrolusite and rhodochrosite. Replacement of Mn by Fe, Pb and Zn, forms various manganiferous or Pb-manganiferous minerals and their pure carbonates, oxides and hydroxides.

Table 2
Chemical assays.

Ag g/m^3	Pb%	Zn%	Fe%	Cu%	Mn%
130.5	1.41	1.59	7.393	0.031	2.74

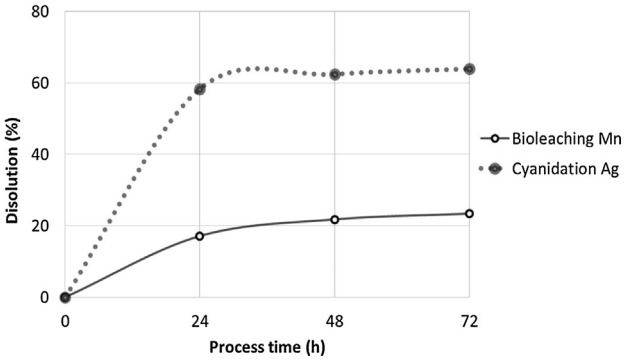

Fig. 1. Manganese dissolution kinetics during the bioleaching process and dissolution kinetics of Ag during the cyanidation processes.

2.3. Microorganism and cultivation conditions

Separation of a native strain from the iron concentrate of *La Encantada* Mine (Durango, Mexico) provides a culture medium of 9 K with a pH of 2 (using H_2SO_4). This medium contains the following compounds: $(NH_4)_2SO_4$ 3.0 g/L, K_2HPO_4 0.5 g/L, $MgSO_4{\cdot}7H_2O$ 0.5 g/L, KCl 0.1 g/L, Ca $(NO_3)_2$ 0.01 g/Land $FeSO_4{\cdot}7H_2O$ 44.2 g/L. Cultivation conditions include temperature of 30 °C, pH of 2.0 and rotational speed of 160 rpm (Dong et al., 2011). The native strain was cultivated and stepwise developed in 100 mL nutrient medium with 10 g iron concentrate, requiring three successive steps to achieve good quality of inoculum.

2.4. Bioleaching process

Bioleaching tests require a 10 L CSTR tank with paddle mixer, to which we add 9 K culture media with a microbial concentration of 10% (v/v). Operation conditions included agitation speed of 700 rpm, 1.5 vvm (temperature and volume of air under standard conditions per volume of liquid per minute) aeration and a constant pH value of 4, solid content of 30%, granulometry of 70% −200 mesh and 72 h retention time. Characterization of the pulp samples every 24 h provides the amount of Mn dissolved in silver.

2.5. Cyanidation process

The pulp obtained from the bioleaching process was washed and leached with sodium cyanide at a concentration of 1000 ppm during 72 h. Samples were extracted every 12 h for rheological characterization and filtered under vacuum (number 42 millipore paper). Analyses of the liquid and solid phases to determine Ag and Mn using atomic absorption spectroscopy also included liquid-phase titration to determine free cyanide using silver nitrate with a rhodanine indicator upon adding potassium cyanide up to the equilibrium point. pH values

Table 1
Mineralogical analysis.

Major (< 30% wt)	Moderate (10%–30% wt)	Minor (2%–10% wt)	Trace (< 2% wt)
Calcite		Quartz, hematite, goethite, loseyite, kaolunite, nepheline	Plumbojarosite dolomite, cerussite, rhodochrosite, oligonite, ilmenite, pyrolusite, fluorite, quenselite, mimetite, blixite, hemimorphite

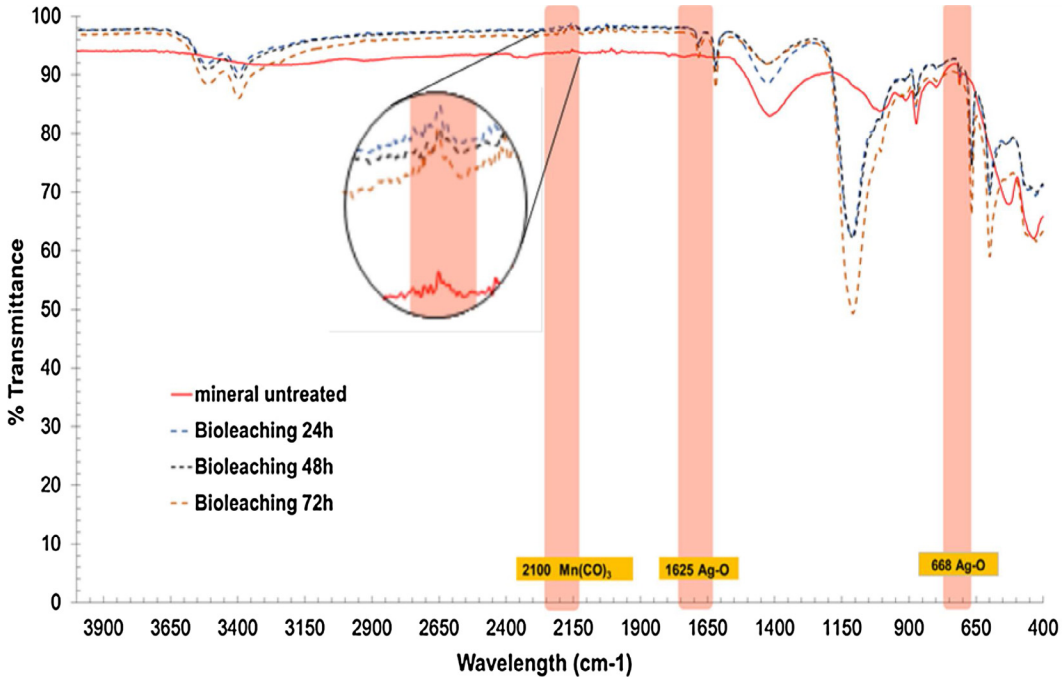

Fig. 2. FTIR spectra for the samples extracted at various times during the bioleaching process.

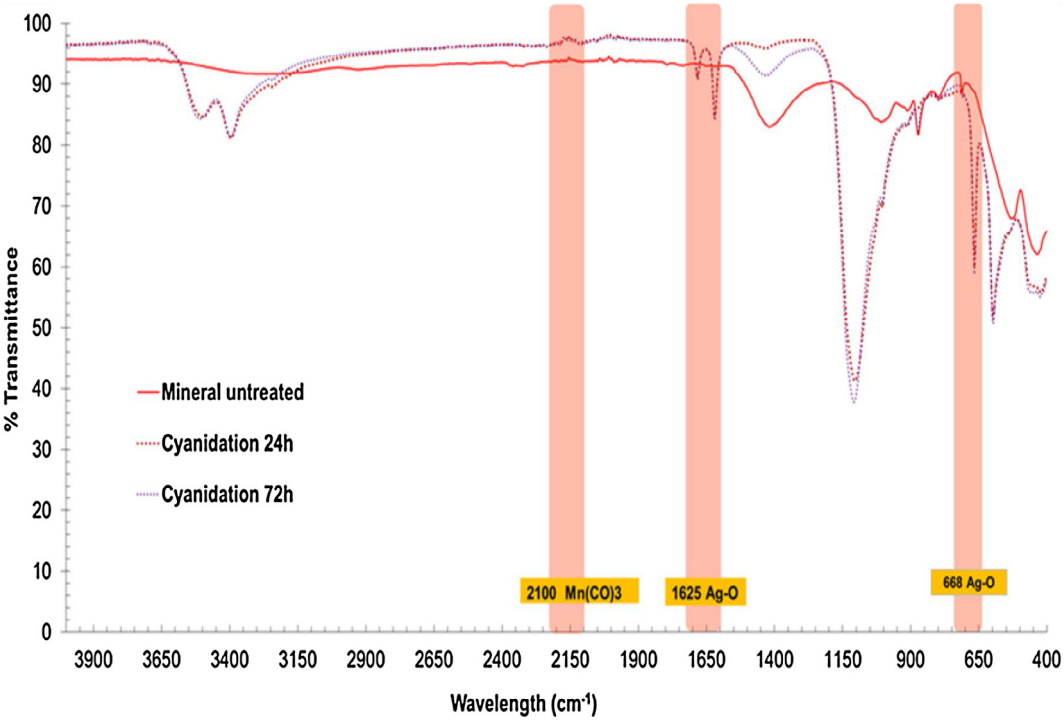

Fig. 3. FTIR spectra for the samples extracted at various times during the cyanidation process.

were kept between 10.5 and 11.0 by adding calcium oxide. Dissolved oxygen rapidly reached saturation values (8 mg/L, approx.) without further change during the leaching process.

2.6. Analysis by infrared spectrometry, (FTIR)

FTIR analysis before and after the bioleaching and cyanidation processes (Nicolet 6700 - diamond point, Thermo Fisher Scientific, USA) employs the potassium bromide disk technique (KBr), providing 100 scans with resolution of 1 cm^{-1}, from 4000 cm^{-1} to 400 cm^{-1}.

2.7. Scanning electron microscopy (SEM)

Microscopy observations follow the method of Medina-Torres et al. (2016). Samples were attached on a copper surface and vacuum-coated with gold at 10 mbar for 90 s (model Desk II, Denton Vacuum, NJ, USA), a scanning electron microscope (JEOL Mod. JSM6300 Jeol, Japan) was used at an accelerating voltage of 20 kV and 1000X magnification.

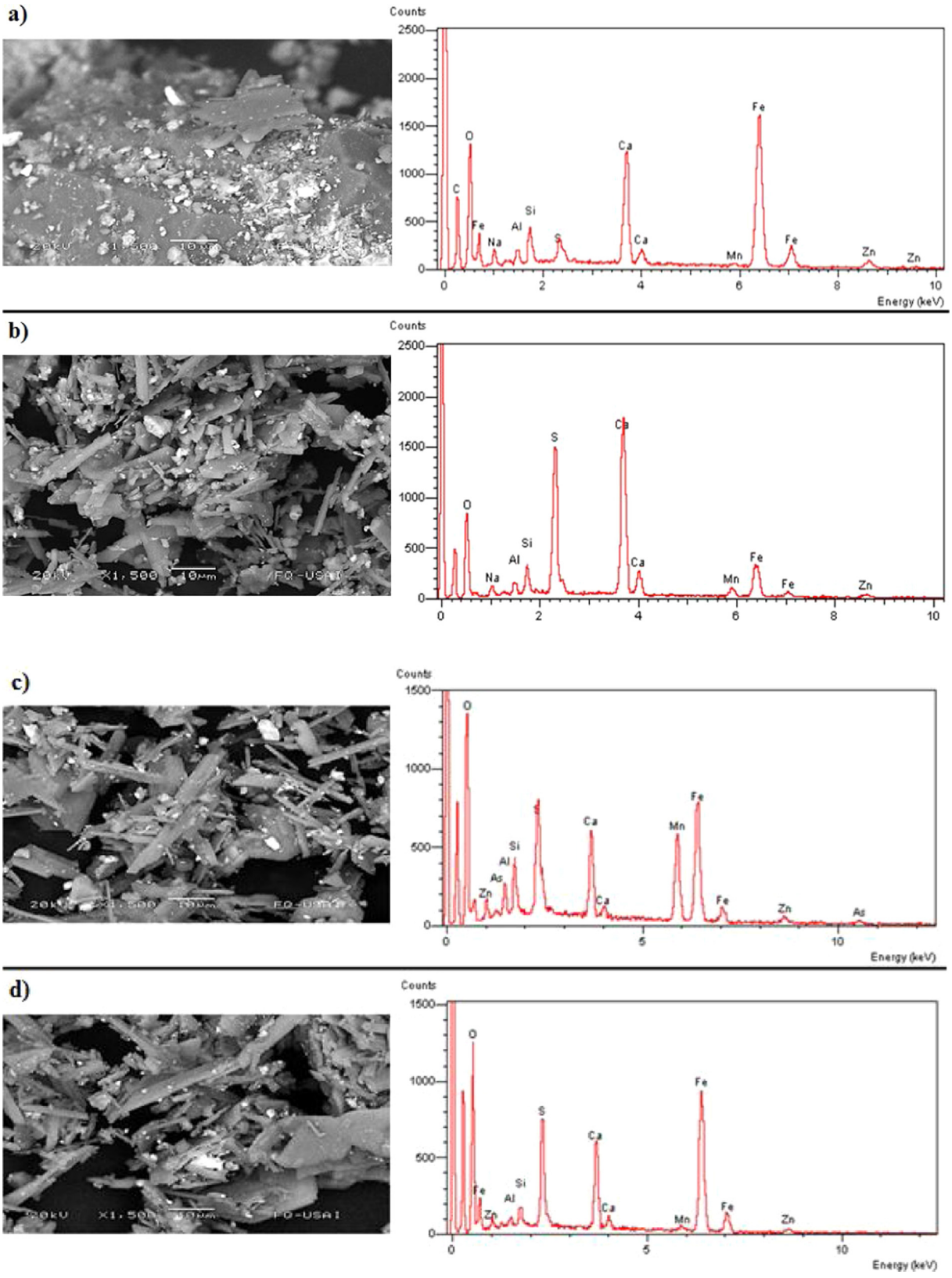

Fig. 4. SEM micrographs and elemental analysis taken at various times during the bioleaching process (a) 0 h, (b) 24 h, (c) 48 h, (d) 72 h.

2.8. Rheology measurements

During the bioleaching process, the method followed includes extraction of samples every 12 h for the rheological characterization. Tests include steady state simple-shear and linear oscillatory flow. A vane geometry was used to prevent sedimentation in a controlled-stress rheometer (AR–G2 TA Instruments), with temperature control (Lab Companio, RW-0525G) at standard temperature conditions of 25 °C. Plots of viscosity η as a function of shear rate $\dot{\gamma}$ under steady state simple-shear flow and plots of the storage (G′) and loss modulus (G″) as

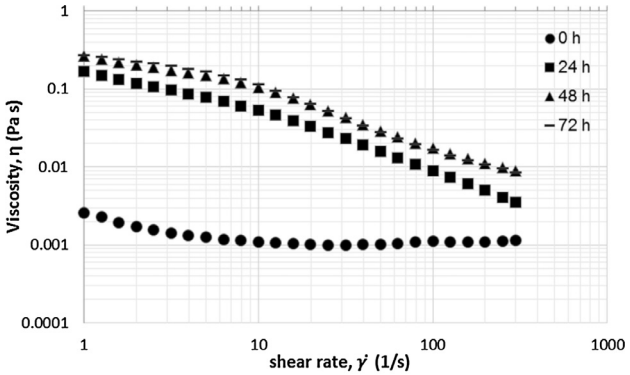

Fig. 5. Steady state simple shear fluid viscosity at various bioleaching times.

functions of frequency under small-amplitude oscillatory flow provide the flow data. The Winter–Chambon criterion estimates the gel point.

3. Results and discussion

3.1. Dissolution kinetics for manganese by bioleaching and silver by the cyanidation process

Fig. 1 shows the dissolution kinetics as a function of process time for Mn in the bioleaching process and for Ag in the cyanidation process. A value of 20–23 wt% of dissolved Mn is reached at 48 h, followed by a constant value up to 72 h. This percentage of bioleached Mn by the catalytic action of microorganisms allows the exposure and liberation of Ag, resulting in a higher dissolution of Ag in the cyanidation process (64%). Accordingly, this evidences that the extraction of Mn from minerals containing 2.74% of Mn and 130.5 g/t of Ag (using the bioleaching process) supports a viable process. This process depends exclusively on an indirect mechanism, namely, that consisting in the intake of the necessary substrate for their metabolic functions from the 9 K medium (specifically from Fe_2SO_4) since the mineral does not assimilate Fe species such as pyrite. The acidic solution of soluble Mn^{2+} results from the oxidizing bacteria from sulfur, whereas the dissolution of non-soluble Mn^{4+} is a product of iron oxidation, which results in the extraction of Mn.

3.2. Analysis by infrared spectrometry, (FTIR)

Fig. 2 shows the FTIR spectra for Ag and Mn in various samples extracted at different times during the bioleaching process. For the case of Ag, typical absorption peaks appear at 1625 y 668 cm^{-1}, which correspond to the Ag -O stretching and deformation bond, respectively. These values are in agreement with those reported in the literature (Rao, 1963). For the untreated mineral, these bonds are not initially present, and their bands appear as the bioleaching process proceeds. This indicates additional amounts of free-Ag present in the culture media as bioleaching proceeds.

The peak at about 3400 cm^{-1} is typical of a hydrogen bond of the water molecule. The fact that the amount of free water in the bioleaching process decreases with the bioleaching time reveals the interaction of the mineral with bacteria, which induces gel formation. The peaks at around 3600 cm^{-1} belong to OH groups of the metals in the suspension, especially iron oxides such as hematite Fe_2O_3 (as shown in Table 2 and in the pronounced peak in Fig. 4) according to the elemental analysis.

The peaks at 1150 cm^{-1} are characteristic of sulfates and ferrous sulfate (Fe_2SO_4), the latter is the main substrate of the 9 K medium responsible for the growth and performance of the ferrous-oxidizing mining bacteria. The spectrum shows the consumption of Fe_2SO_4, especially between 24 and 48 h, corresponding to the large catalytic activity of the bacteria and high dissolution of Mn.

A low amount of Mn (2.74%) is usually present as *Rhodochrosite* mineral ($MnCO_3$) with typical absorption peaks at 2100 cm^{-1}, as reported in the literature (Reed and Duncan, 2010). If this quantity is sufficiently large, the mineral interacts with silver and the extraction of silver becomes more difficult. Fig. 2 (with a zoom in the inset) shows the very small absorption bands of Mn, while for the case of the cyanidation process, Fig. 3 depicts the FTIR spectra for samples extracted at different times during the cyanidation process, revealing the amount of silver exposed and released during the previous bioleaching step. The pronounced adsorption peaks of silver exceed in magnitude those of the bioleaching step, evidencing that the silver is ready for extraction at the first 24 h of the cyanidation process.

3.3. Scanning electron microscopy (SEM) and infrared spectroscopy (IR)

Fig. 4a–d shows micrographs with their corresponding elemental analysis of the bioleaching process at various times. Micrographs depict mineral surface modification as the bioleaching process evolves,

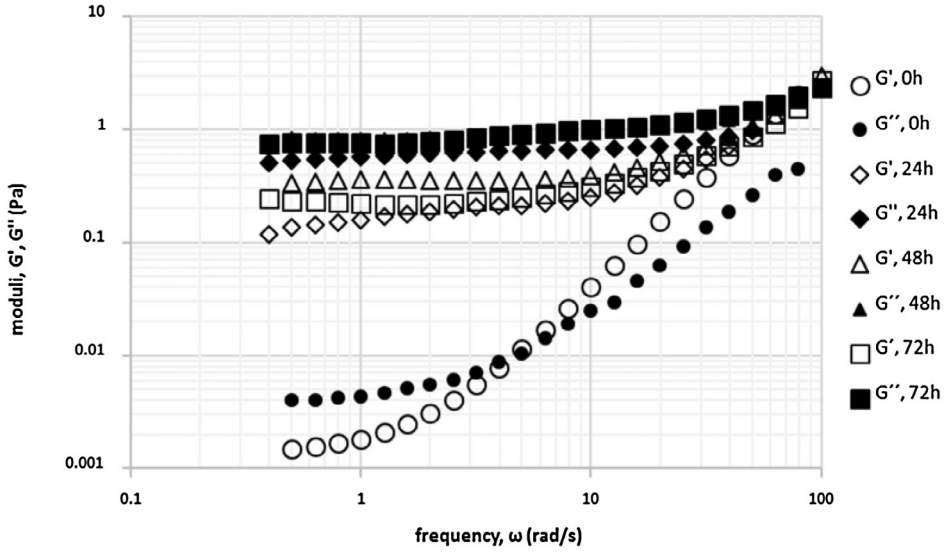

Fig. 6. Dynamic moduli in small amplitude oscillatory shear flow (SAOS) of samples extracted at various times during the bioleaching process.

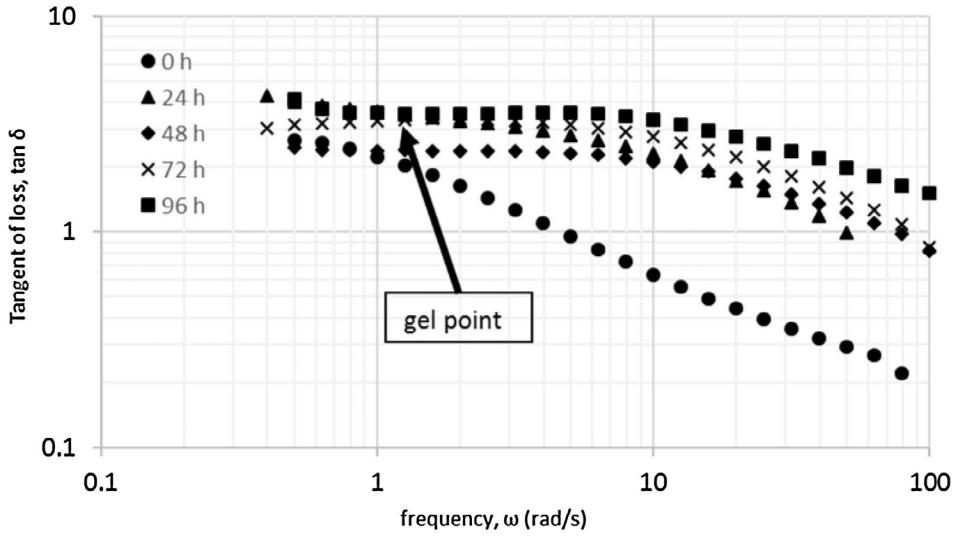

Fig. 7. Tangent of the phase angle as a function of the frequency for the mineral pulp extracted at various bioleaching process times.

consisting in a fibrous morphology attributed to corrosion and wearing by the action of microorganisms on the mineral surface. At 48 h, an intense peak related to Mn content in the elemental analysis appears, after which bands decrease in intensity consistently with the dissolution kinetics presented in Fig. 1. Tributsh (2010) reported surface wearing in sulfur minerals caused by chemicals produced by EPS bacteria. Findings in biological bioleached media of phospholipids in the exopolyssacharides (identified as bioleaching agents) acting as sulfur surfactants (surface activator) reveal apparent agreement with the mechanism exposed here. A 9 K media is essential to increase the total ferric sulfate demand (since the mineral does not contain Fe species such as pyrite). Iron mineral and dissolved sulfur of the 9 K medium promotes the oxidation of Fe^{2+} ions to Fe^{3+} and the production of sulfuric acid by the catalytic action of the bacteria (as an indirect bioleaching process) resulting in dissolution of the mineral matrix and thus releasing and exposing the silver content (*rodhochrosite*), as confirmed by SEM analysis.

3.4. Rheology

3.4.1. Steady state simple-shear

Fig. 5 shows the shear viscosity of the mineral pulps for various bioleaching times. At the beginning of the bioleaching process (0 h), the pulp viscosity is almost that of water, due to sedimentation of solid particles (He et al., 2004). As the bioleaching evolves, viscosity increases at 24 h, evidencing the production of soluble bacteria in the media with the consequent increase in the exopolysaccharides content. At 48 h, the viscosity of the pulp reaches a maximum attributed to the maximum concentration of exopolysaccharides in the medium. These results are in accordance with the dissolution kinetics presented in Fig. 1; the steep increase in viscosity has also been reported for concentrated (57 wt%) aqueous dispersions of reactive particles of muscovite clay mineral (Nosrati et al., 2011). In this case, the media behaves as a shear-thinning fluid during the whole bioleaching process. Other factors also contribute to the complex rheological behavior of the pulp, such as changes in pH, particle size reduction by wearing and corrosion, and the change in density of the media and particles. These factors result in flow phenomena such as thixotropy, yield stress, rheopexy, as reported elsewhere for aging mineral suspensions (Nosrati et al., 2011).

3.4.2. Dynamic spectra in small amplitude oscillatory shear flow (SAOS)

Fig. 6 displays the SAOS spectra of samples extracted at various times during the bioleaching process. At time 0 h, the moduli attach low values with the viscous modulus (G″) dominating over the elastic modulus (G′). This is an expected result, since the material is predominantly viscous with viscosity similar to water, as observed in Fig. 5. At 24 h, moduli have increased 2 orders of magnitude as compared to those at 0 h. Again, the viscous modulus dominates along the entire frequency range. The system behaves as a soft gel with *solid-like* behavior as the moduli become independent of frequency. The weak gel behavior appears due to the short-range interactions between bacteria and the solid particles or particle-particle interactions in the mineral pulp. The maximum in the moduli appears at 48 h, consistently with the shear viscosity results of Fig. 5. Nosrati et al. (2011) reported similar results for aging mineral pulps; where in a rapid increase in the viscoelastic moduli with aging time produces a gel in the 57 wt% aqueous suspensions of muscovite clay mineral. Data shows a crossover point (G′ = G″) at high frequency (around 100 rad/s), while data corresponding to 0 h depicts a crossover point at 4 rad/s, approximately.

Finally, Fig. 7 shows SAOS data in terms of tan δ (phase angle) as a function of frequency. The crossover point appears, corresponding to tan δ = 1 (G′ = G″). Constant values at low frequencies appear, except the curve at 0 h. According to the Winter and Chambon criterion, the gel point is the crossover point of the phase angle curves, corresponding to a value of $\tan\delta = 5$ at a frequency of $\omega = 1.259\ \left(\frac{rad}{s}\right)$,which renders a value of the gel constant $S = 0.0171\ Pa\ s^n$ (Winter and Chambon, 1986) which is characteristic of a weak gel.

4. Conclusions

In this work, analysis of silver manganese pulps during the bioleaching and cyanidation processes included dissolution kinetics, FTIR, morphology, and rheological tests. The dissolution kinetics revealed that manganese dissolves up to 23% at 48 h process time, allowing the exposure and liberation of silver from the mineral ore and thus increasing the extraction and diminishing the cyanide used during the cyanidation process.

Validation of the silver exposure appears in the FTIR spectra of samples extracted at different cyanidation times. The mineral pulp behaves as a shear-thinning fluid with a complex rheology which changes during the bioleaching process attaining a maximum viscosity at 48 h process time.

The mineral pulp is a viscoelastic material with predominant viscous behavior but with *solid-like* characteristics and weak gel response according to the Winter-Chambon criterion.

Results of this bioleaching process shed light on the optimization and extraction of Ag, diminishing the cyanide amount used during the

conventional cyanidation process. The increase in viscosity attained during the bioleaching process has an important effect on the power consumption of mixing, because of the larger amount of time (days) needed for these bioprocesses.

Acknowledgements

We acknowledge the financial support from CONACYT through the project 235880.

References

Boger, D.V., 2000. Rheology and the minerals industry. Mineral Process. Extractive Metallurgy. Rev.: Int. J. 20, 1–25.
Cerpa, A., García-González, M.T., Serna, C.J., Tartaj, P., 2001. Relationship between the colloidal and rheological properties of mineral suspensions. Can. J. Chem. Eng. 79, 608–611.
Cerpa, A., Garcell, L.R., 1998. Propiedades superficiales y reológicas de suspensiones minerales lateríticas. Evento Metalurgia'98, Abstracts, Ciudad de La Habana.
Cerpa, A., Tartaj, P., García-González, M.T., Requena, J., Garcell, L., Serna, C.J., 1999. Mineral- content and particle size effects on the colloidal properties of concentrate lateritic suspensions. Clays Clay Miner. 47, 515–530.
Dong, Y.B., Lin, H., Wang, H., Mo, X.L., Fu, K.B., 2011. Effects of ultraviolet mutation on bioleaching of low-grade copper tailings. Miner. Eng. 24, 871–875.
Erüst, C., Akcil, A., Sekhar, G.C., Tuncuk, A., Deveci, H., 2013. Biohydrometallurgy of secondary metal resources: a potential alternative approach for metal recovery. J. Chem. Technol. Biotechnol. 88, 2115–2132.
Garcell, L.R., 2001. Flujo por tuberías de suspensiones minerales no newtonianas. Universidad de Oriente, Monografía.
Garcell, L.R., 2004. Sedimentación de suspensiones minerales: influencia de las propiedades superficiales y reológicas sobre el proceso. Facultad de Ingeniería Química, Universidad de Oriente, Santiago de Cuba.
He, M., Wang, Y., Forssberg, E., 2004. Slurry rheology in wet ultrafine grinding of industrial minerals: a review. Power Technol. 147, 94–112.
Medina-Torres, L., Calderas, F., Femenia, A., Sánchez-Olivares, G., Gónzalez-Laredo, F.R., Santiago-Adame, R., Núñez-Ramírez, D.M., Rodríguez-Ramírez, J., Manero, O., 2016. Structure preservation of Aloe vera (barbadensis Miller) mucilage in a spray drying process. LWT-Food Sci. Technol. 66, 93–100.
Ndlovu, B., Becker, M., Forbes, E., Deglon, D., Franzidis, J.P., 2011. The influence of phyllosilicate mineralogy on the rheology of mineral slurries. Miner. Eng. 24, 1314–1322.
Nosrati, A., Addai-Mensah, J., Skinner, W., 2011. Rheology of aging aqueous muscovite clay dispersions. Chem. Eng. Sci. 66, 119–127.
Patra, P., Nagaraj, D.R., Somasundaran, P., 2010. Impact of pulp rheology on selective recovery of value minerals from ores. In: Singh, R., Das, A., Banerjee, P.K., Bhattacharyya, K.K., Goswami, N.G., (Eds.), © NML Jamshedpur. (MPT-2010). Proceedings of the XI International Seminar on Mineral Processing Technology, pp. 1223–1231.
Pérez, G.L., 2004. Efecto de la temperatura y de la distribución de tamaño de las partículas sobre la correlación entre las propiedades reológicas y coloidequímicas de las suspensiones lateríticas. Universidad de Oriente, Santiago de Cuba, pp. 73 [Tesis de Maestría].
Rao, C.N.R., 1963. Chemical applications of infrared spectroscopy. Academic Press, New York and London. http://dx.doi.org/10.1126/science.144.3625.1441. 19, 144, 683.
Reed, Z.D., Duncan, M.A., 2010. Infrared spectroscopy and structures of manganese carbonyl cations, $Mn(CO)_n$ (n = 1–9). J. Am. Soc. Mass Spectrom. 21, 739–749.
Rivas, S., Colás, E., 2005. Efecto de la granulometría sobre la reología de suspensiones de Cieno Carbonatado. Universidad de Oriente, Santiago de Cuba, tesis-diploma, pp. 61.
Ruas-Maiedo, P., de los Reyes-Gavilán, C., 2005. Invited Review: methods for the screening, isolation, and characterization of exopolysaccharides produced by lactic acid bacteria. J. Dairy Sci. 88, 843–856.
Sandström, Å., Petersson, S., 1997. Bioleaching of a complex sulphide ore with moderate thermophilic and extreme thermophilic microorganisms. Hydrometallurgy 46, 181–190.
Sofrá, F., Boger, D.V., 2002. Environmental rheology for waste minimisation in the minerals industry. Chem. Eng. J. 86, 319–330.
Tributsh, H., 2010. Direct versus indirect bioleaching. Hydrometallurgy 59, 177–185.
Winter, H.H., Chambon, F., 1986. Analysis of Linear Viscoelasticity of a Crosslinking Polymer at the Gel Point. Massachusetts, EE. UU: Department of Chemical Engineering and Department of Polymer Science and Engineering, Amherst.
Zamora, N.L., 2003. Caracterización reológica de los cienos carbonatados que se manejan industrialmente en Moa. ISPJAM, Santiago de Cuba, Trabajo de Diploma, pp. 59.
Zhang, M., Peng, Y., 2015. Effect of clay minerals on pulp rheology and the flotation of copper and gold minerals. Miner. Eng. 70, 8–13.